EUROPHYSICS LETTERS 10 March 1997

Europhys. Lett., **37** (8), pp. 517-522 (1997)

Collapse and revival of the fringe pattern in a multiple-beam atom interferometer

M. Weitz, T. Heupel and T. W. Hänsch

Max-Planck-Institut für Quantenoptik - 85748 Garching, Germany

(received 11 November 1996; accepted in final form 30 January 1997)

PACS. 03.75Dg – Atom and neutron interferometry.
PACS. 42.50Vk – Mechanical effects of light on atoms, molecules, electrons, and ions.
PACS. 32.80Lg – Mechanical effects of light on atoms, molecules, and ions.

Abstract. – We report on the observation of collapse and revival of the fringe pattern in a multiple-beam atom interferometer, when the drift time between the beam splitting processes is varied. The atomic beam splitters are realized with laser pulses pumping the atoms into velocity selective dark states. For small drift times, the interference signal shows the sharply peaked Airy function-like pattern characteristic for multiple-beam interference. The fringe pattern collapses for larger drift times due to a recoil phase shift increasing quadratically with the transverse atomic momentum. When the total interaction time reaches an integer multiple of the inverse two-photon recoil energy in frequency units, the original fringe pattern is revived.

In recent years, we have witnessed a rapid progress in the field of interferometry with neutral atoms [1]. Atom interferometers are developing into very sensitive probes for acceleration and rotation, and can be used for measurement of the photon recoil energy of an atom. In a previous paper, we have reported on an atom interferometer with multiple paths [2]. Compared to conventional two-beam atom interferometers where sinusoidal fringes are observed, the interference signal here shows a more sharply peaked Airy function-like fringe pattern known, *e.g.*, from optical Fabry-Perot interferometers.

We report here on the observation of collapse and revival of the fringe pattern in a multiple-beam atom interferometer, when the drift time of the atoms between the beam splitting processes is varied. While good contrast of the interference pattern is observed for small drift times, the contrast drastically decreases when the drift time approaches a critical time determined approximately by the inverse kinetic energy difference between a central and an extreme outermost interfering path in frequency units. A collapse of the fringe pattern does not occur for most common optical multiple-beam interference experiments (*e.g.*, a Fabry-Perot resonator), where the phase difference between adjacent paths is constant for all paths. In the atom interferometer discussed here optical pulses act as atomic beamsplitters and transfer transverse momentum to the atom in units of two-photon recoils. Besides a usual linear phase term, an additional phase associated with the photon recoil energy quadratic in transverse atomic momentum appears, which can be understood intuitively by considering the kinetic-

energy differences between the paths. As the accumulated quadratic recoil phase between a central and the outermost paths of the interferometer approaches unity for larger drift times, the fringe pattern collapses.

At first sight, one therefore might be pessimistic about the possibility to perform precision measurements with such a multiple-beam atom interferometer, since a high sensitivity to inertial fields naturally requires large drift times. As was predicted previously [2], the original fringe pattern is however revived when the accumulated quadratic phase between all adjacent interferometer paths reaches an integer multiple of 2π.

Both collapse and revival of the fringe pattern are demonstrated here for the first time in a multiple-beam interferometer based on three laser pulses pumping the atom into multilevel dark states. In this way we prove the existence of this fundamentally interesting effect, which is not observed in most two-beam atom interferometer geometries, and we demonstrate the feasibility of multiple-beam atom interferometers with large drift times, as necessary for precision experiments.

Collapse and revival effects similar to those described have long been observed in classical optics starting with Talbot's discovery of self-imaging of periodic objects [3]. There, such phenomena are near field effects, and can be explained by solving the wave equation and including all terms up to quadratic order in the phase, which is known as the Fresnel approximation. More recently, Clauser and Li [4] have taken advantage of the Talbot effect in an atom interferometer based on three mechanical gratings. For revival times in their experimental implementation the signal arises predominantly from many two-beam atom interferometers of different initial momentum adding up incoherently to an enhanced total signal. Further, self-imaging of an atom diffraction grating has been observed [5]. The Talbot effect has found applications in the subrecoil laser cooling of atoms [6]. Very recently, multiple-beam interference of atoms has also been realized by recombining the diffraction pattern of an off-resonant standing wave [7]. In this approach somewhat complementary to ours, the interference is detected via the signal change when sweeping the drift time through the revival times.

The scheme of our experiment is as follows. Atoms from a cesium atomic beam are irradiated by a sequence of three optical interferometer pulses of two counterpropagating beams in a σ^+-σ^- polarization configuration, as shown in fig. 1. Generally, a multiple-beam atom interferometer with N paths can be realized using an atom with a transition from a ground state of total angular momentum $F = N - 1$ to an excited state with total angular momentum $F' = F$. Here, the light is tuned to the $6S_{1/2}(F = 4)$-$6P_{1/2}(F' = 4)$ transition of the cesium $D1$ line.

The first laser pulse projects each atom onto a nonabsorbing "dark" coherent superposition of the $N = 5$ even magnetic ground-state sublevels ($m_F = -4, -2, \ldots, 4$), where each sublevel is associated with a distinct relative momentum. The remaining atoms are mostly pumped into the $F = 3$ hyperfine level, which is not detected any more. At a time t after the pulse, the dark state in $F = 4$ has evolved into

$$|\varphi_D(t)\rangle = \sum_{n=0}^{N-1} w_n e^{-it\delta_n} |g_{2n-N+1}, \mathbf{p} + n\,\hbar(\mathbf{k}_+ - \mathbf{k}_-)\rangle\,, \tag{1}$$

where $|g_{m_F}, \mathbf{p}_n\rangle$ denotes a ground state of magnetic quantum number m_F and momentum $\mathbf{p}_n$. Further, $\mathbf{k}_\pm$ are the wave vectors of the σ^+ and σ^- polarized waves. We assume equal field amplitudes for both laser fields at all times. The weights w_n are chosen such that $|\varphi_D(t)\rangle$ is dark at $t = 0$. The Raman-like two-photon detunings δ_n are

$$\delta_n = n\left(\omega_+ - \omega_- - \omega_\mathrm{A} - \frac{(\mathbf{k}_+ - \mathbf{k}_-)\cdot\mathbf{p}}{m}\right) - n^2\omega_\mathrm{r}\,, \tag{2}$$

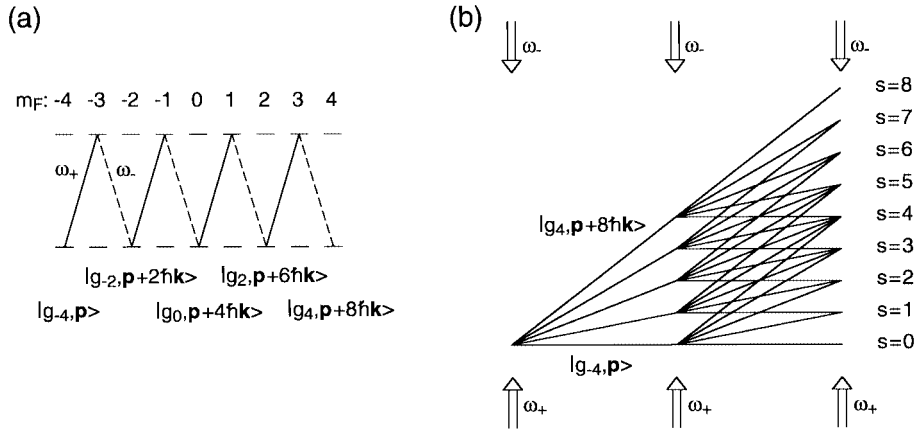

Fig. 1. – *a*) Level scheme and *b*) outline of an atomic multiple-beam interferometer. The different families of interfering wave packets are numbered as $s = 0, \ldots, 8$.

where $\omega_\pm = c|\mathbf{k}_\pm|$, ω_{A} denotes the splitting between two adjacent even-m_F levels, and $\omega_{\mathrm{r}} = \hbar(\mathbf{k}_+ - \mathbf{k}_-)^2/2m$ the recoil energy of a two-photon transition in frequency units. For $N > 2$ the dark state is never fully stationary when $\mathbf{k}_+ \neq \mathbf{k}_-$, since the detunings δ_n cannot be tuned to zero simultaneously for $\omega_{\mathrm{r}} > 0$. This leakage, however, is negligible for sufficiently short optical pulses. The recoil term quadratic in n also causes the collapse and revivals of the fringe pattern.

At the time of the second laser pulse the atomic wave packet has separated into five paths with well-defined relative momentum and m_F quantum number. The second pulse will again project each packet onto a dark state and optically pump the remaining atoms into the $F = 3$ level. By this projection the second pulse splits each of the five separate paths again into five. Finally at a time T after the second pulse when several atomic wave packets spatially recombine, a third optical pulse closes the atom interferometer. We then detect the number of atoms found in the dark state as a function of the phase of the final pulse. With no additional phase and for $\omega_{\mathrm{r}}T = r\pi$ with r as an integer, the third pulse leaves the atoms in the dark state (in $F = 4$), since the atom is already dark for the light field. When, *e.g.*, the phase is varied less $F = 4$ ground-state population is detected, since the atom then couples to the light during the third pulse and is optically pumped into the $F = 3$ hyperfine ground state.

We now assume an initial transverse (along $\mathbf{k}_+ - \mathbf{k}_-$) atomic-momentum spread Δp_z with $\Delta p_z\ |\mathbf{k}_+ - \mathbf{k}_-|T/m \gg 1$, which intrinsically is present for a spatially sufficiently well-localized atomic wave packet to allow a clear spatial separation of the different wave packets within the interferometer. The calculation of the interferometer fringe pattern has been described previously [2], and gives the following probability for an atom to remain in the uncoupled state after the optical pulses as a function of the phase of the final pulse $\delta\theta$:

$$\big|\,|\Psi\rangle\big|^2 = \sum_{s=0}^{2N-2} \big|\,|\Psi_s\rangle|^2\,, \tag{3}$$

where

$$|\Psi_s\rangle = \sum_q w_{s-q^2} w_q^2 \exp\left[i(q\delta\theta + (sq - q^2)2\omega_{\mathrm{r}}T)\right] |\varphi_{D,s}\rangle\,. \tag{4}$$

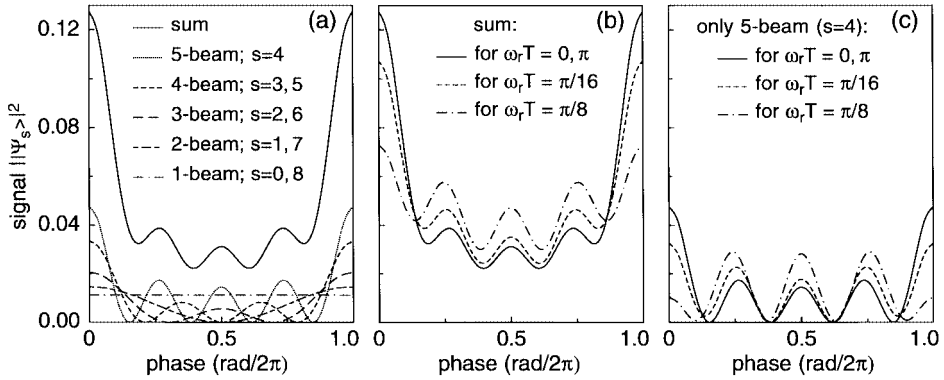

Fig. 2. – Calculated interference pattern (ratio of atoms found in a dark state after the optical pumping pulses and those initially in the dark state) of the atomic multiple-beam interferometer as a function of the phase of the third optical pulse. *a*) Interference signal for drift times T at revival times $T = r\pi/\omega_r$, where r is an integer. Both the contributions of the different families of interfering wave packets ($s = 0, \ldots, 8$) and the total (sum) signal is shown. *b*) Calculated total signal and *c*) signal for only the family with five interfering wave packets for different drift times T.

Each wave function $|\Psi_s\rangle$ corresponds to a family of interfering wave packets which spatially recombine at the time of the third interferometer pulse, as shown in fig. 1*b*). The $|\varphi_{D,s}\rangle$ denote the corresponding dark states at this time. The index q numbers the interfering paths in each family, and runs from $\max(0, s - N + 1)$ to $\min(N - 1, s)$.

The interference signals of the different families add incoherently to the total signal. The sum and the contributions are shown in fig. 2*a*) for drift times close to revival times ($\omega_r T = r\pi$), when the recoil term in eq. (4) can be neglected. The family with $s = 4$ and five interfering beams gives the sharpest principal maxima, and also contributes most to the total signal. Figure 2*b*) shows the calculated total interference signal for different drift times. Far from revival times a clear decrease of the fringe contrast is observed. As an example for the signal from an individual family of interfering wave packets, fig. 2*c*) shows the signal of only the family with five beams ($s = 4$) for different drift times. Similar to the total signal, collapse and revival of the fringe pattern is predicted.

To explore the possibility of inertial measurements with this atom interferometer, assume

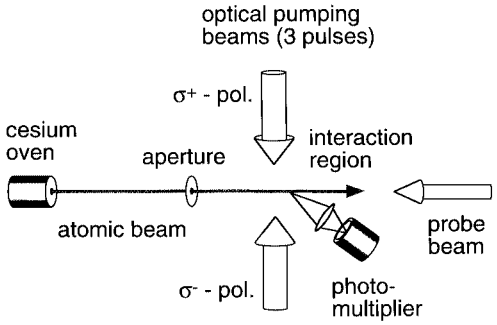

Fig. 3. – Scheme of the experimental setup for a multiple-beam atomic interferometer.

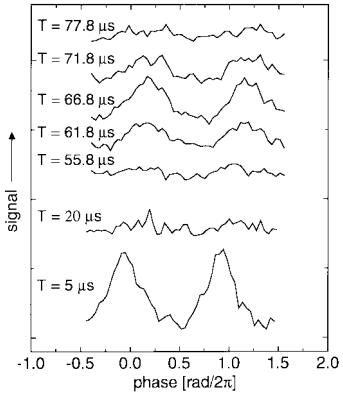

Fig. 4. – Typical signals of the multiple-beam atomic interferometer shown in fig. 1 as a function of the phase of the third optical pulse. For drift times T between successive pulses above a few μs the fringe pattern collapses due to a recoil phase shift increasing quadratically with the path number. When T reaches the first revival time at $\pi/\omega_r \cong 66.8$ μs, a revival of the fringe pattern is observed. The fringe pattern again collapses for even larger times T. Note that the data set with T above 50 μs had to be taken with a higher photomultiplier supply voltage.

now that the atom is subject to an acceleration $\mathbf{g}$, or the interferometer is rotated with an angular velocity Ω. The obtained interferometer signal can be derived by considering the variation of the laser difference frequency in the frame of an atom with initial velocity $\mathbf{v}$ [8]. The term $\omega_+ - \omega_-$ in eq. (2) is replaced by $\omega_+ - \omega_- - (\mathbf{k}_+ - \mathbf{k}_-) \cdot \mathbf{g}t - (\mathbf{k}_+ - \mathbf{k}_-) \cdot \Omega \times \mathbf{v}t$. The corresponding interferometer signal can be obtained by replacing the phase $\delta\theta$ with $\delta\theta - (\mathbf{k}_+ - \mathbf{k}_-) \cdot \mathbf{g}T^2 - (\mathbf{k}_+ - \mathbf{k}_-) \cdot \Omega \times \mathbf{v}T^2$ in eq. (4). The interference signal is shifted uniformly, and the degree of rotation or acceleration can be determined.

Our experimental setup shown in fig. 3 is similar to that used in our previous work [2]. It has been improved to allow sufficiently long drift times for an observation of collapse and revival mainly by Doppler selection of slower atoms from the thermal atomic beam.

The beam of cesium atoms effuses from an oven in a vacuum chamber. The atoms enter an optical interaction region that is magnetically shielded by a Mu-metal tubing with a homogeneous 9 mG magnetic bias field oriented along the optical-pumping beams. A series of three optical-pumping pulses is irradiating the atoms. The pulses are generated from a Ti:sapphire laser operating near 894 nm. After passing a first acousto-optical modulator used as a fast optical switch, the light is split to provide the two counterpropagating optical-pumping beams. Both beams then pass a further acousto-optical modulator, are spatially filtered and expanded to Gaussian beam diameters of 43 mm before entering the atomic-beam apparatus.

The population left in the dark state after the optical pumping pulses is measured by applying a further laser pulse tuned to the $6S_{1/2}(F = 4)$-$6P_{3/2}(F' = 5)$ cycling transition and detecting the resulting fluorescence. This probe beam is generated by a diode laser, and propagating in opposite direction to the atomic beam to allow Doppler selection of only a part of the thermal atomic velocity distribution. While the most probable atomic velocity is 290 m/s, the detection laser is tuned to address atoms moving at 140 m/s. Use of this detection method allows a significant increase of the interferometer drift time, since Doppler selection also efficiently suppresses signal contributions from those atoms moving far above the most probable atomic velocity.

In a typical pulse sequence we start with a 1.2 μs long period of lower light intensity for the optical-pumping beams to select a velocity slice of about 200 kHz Doppler width in a direction along the optical pumping beams from the initial transverse beam velocity distribution of

1.2 MHz Doppler width (these values refer to the width for a Raman-like two-photon transition). The beam power is then increased to full value (about 40 mW/cm^2 in the beam center) for 0.8 μs. The typical length of the second and third interferometer pulse is 1.2 μs. Subsequently, the population in the dark state is measured. The phase of the third optical-pumping pulse can be changed by varying the phase of the rf drive frequency of the acousto-optical modulator in one beam (*e.g.*, that with frequency ω_+). The typical repetition rate of the pulse sequence is 3.5 kHz. We alternate between a sequence with the phase of the light of frequency ω_+ shifted in the final pulse and one with no additional phase. The difference in the population left in the dark state after the interferometer pulses is determined with a lock-in amplifier.

Typical experimental interferometer signals are shown in fig. 4 for different drift times T between the pulses. For drift times T above a few μs the fringe pattern collapses. When the drift time however approaches the first revival time at $T = \pi/\omega_r$ (equals 66.8 μs), fringes again become clearly visible and reach maximum contrast at the revival time. For somewhat larger drift times we again observe a collapse of the fringe pattern. Note that while the signal of atoms in the dark state as monitored here increases in the interference maxima, the fluorescence signal scattered during the final pulse, as detected in our previous work [2], decreases in interference maxima.

The observed width of the principal maxima typically is $0.32 \cdot 2\pi$ for small drift times ($T = 5$ μs). This width increases for larger drift times to $0.36 \cdot 2\pi$ at the first revival time. Both values are clearly above the theoretical width of $0.18 \cdot 2\pi$, but still considerably below the value $0.5 \cdot 2\pi$ observed in a two-beam atom interferometer.

To determine the cause of the fringe broadening, we have studied Doppler-free multilevel Ramsey interference fringes [2]. The typical observed fringe width for this setup with magnetic shielding was $0.20 \cdot 2\pi$ at a drift time of 130 μs, which is reasonably close to the theoretical value of $0.16 \cdot 2\pi$. We therefore do not ascribe much broadening of the interferometer signal to inhomogeneous stray magnetic fields. We attribute the experimental broadening to be mainly due to both the large initial atomic velocity spread parallel to the laser beams and to imperfect optical wave fronts.

To conclude, we report on the observation of collapse and revivals of the interference fringes in a multiple-beam atom interferometer. For future experiments, use of laser-cooled cesium atoms in an atomic fountain will allow both longer interferometer drift times up to $T = 200$ ms and narrower fringe widths. Precision measurements of, *e.g.*, gravitation and rotation should be possible with an increased sensitivity.

REFERENCES

[1] See, for example, Berman P. (Editor), *Atom Interferometry* (Academic Press) in press.
[2] Weitz M., Heupel T. and Hänsch T. W., *Phys. Rev. Lett.*, **77** (1996) 2356; Weitz M., Heupel T. and Hänsch T. W., *Verhandl. DPG (VI)*, **31** (1996) 258.
[3] Patorski K., *Progress in Optics XXVII*, edited by E. Wolf (North-Holland, Amsterdam) 1989.
[4] Clauser J. F. and Li S., *Phys. Rev. A*, **49** (1994) R2213.
[5] Chapman M. S. *et al.*, *Phys. Rev. A*, **51** (1995) R51.
[6] Sander F., Devolder T., Esslinger T. and Hänsch T. W., submitted to *Phys. Rev. Lett.*
[7] Cahn S. B., Kumarakrishan A., Shim U. and Sleator T., to be published.
[8] Kasevich M. and Chu S., *Appl. Phys. B*, **54** (1992) 321.